

Bound and resonance states near the critical charge region in two-electron atomsLi Guang Jiao * and Ruo Yu Zheng*College of Physics, Jilin University, Changchun 130012, People's Republic of China*Aihua Liu †*Institute of Atomic and Molecular Physics, Jilin University, Changchun 130012, People's Republic of China*H. E. Montgomery, Jr. *Chemistry Program, Centre College, Danville, Kentucky 40422, USA*

Yew Kam Ho

Institute of Atomic and Molecular Sciences, Academia Sinica, Taipei 10617, Taiwan

(Received 21 December 2021; accepted 26 April 2022; published 11 May 2022)

The critical nuclear charge Z_c of the two-electron atoms below which the ground state transforms into a shape resonance and the critical stability of the system around Z_c have been well established. However, the behavior of the shape resonance below Z_c is still a mystery. By employing the complex-scaling method using Hylleraas configuration-interaction basis functions, we trace the trajectory of the shape resonance from Z_c down to a very small nuclear charge. It is shown that at specific values of Z far below Z_c the resonance crosses over higher-lying one-electron thresholds, and when Z is decreased below 0.316, the shape resonance lies above the three-body breakup threshold. We finally show that the imaginary part of the resonance energy at small nuclear charges can be modeled by the dispersion relation with a high-order Padé approximant correction.

DOI: [10.1103/PhysRevA.105.052806](https://doi.org/10.1103/PhysRevA.105.052806)**I. INTRODUCTION**

The critical stability and asymptotic behavior of atomic systems with varying nuclear charge have long been of great interest due to their important roles in our understanding of quantum phase transitions and symmetry breaking of electronic configurations [1–3]. Research of particular interest is focused on, for example, the application of $1/Z$ perturbation-expansion theory in atomic isoelectronic sequences [4–7], the interpretation of static correlation energy and the symmetry-adapted (symmetry-broken) property in the restricted (unrestricted) Hartree-Fock solutions [8–11], and the critical nuclear charge Z_c of a general N -electron system, at which all bound states cease to exist [12–17]. The two-electron atom which explicitly includes interelectronic correlation and possesses critical stability around the corresponding critical nuclear charge provides us an ideal prototype for research on more complex atoms.

A systematic investigation of the electronic correlation effect in calculating the binding limit for two-electron atoms is available in Stillinger and Weber's classic 1974 paper [18]. Since then, the determination of the exact value of Z_c has become a subject of wide interest. The milestone of predicting Z_c with high accuracy and analyzing its analytic property as an essential singularity was performed by Baker *et al.*

[5] based on an extensive variational perturbation calculation of the coefficients in the $1/Z$ expansion of system energy. Their estimated value of $Z_c = 0.91103$ was later improved to 0.91102826 by Ivanov [19] using a different fitting procedure and confirmed alternatively to be 0.911029 by Neirrotti *et al.* [20] employing the finite-size scaling method. Two subsequent works made significantly different predictions about both the value of Z_c and its nature of singularity. They are the convergence study of the $1/Z$ expansion by Zamastil *et al.* [6] and the direct variational calculation of Guevara and Turbiner [14], who gave estimates of $Z_c = 0.90223$ and 0.910850, respectively. They both claimed that the singularity at Z_c is a branch point with exponent $3/2$. This discrepancy was unambiguously resolved by the triple-set Hylleraas-basis calculation of Estienne *et al.* [21], whose prediction of $Z_c = 0.91102822407725573$ still serves as the benchmark value. Subsequently, this result was reproduced for the leading 11 decimal digits by Olivares-Pilón and Turbiner [22] with the help of the Lagrange-mesh method and for 12 digits by Karr [23] based on explicitly correlated Sturmian wave functions. It is worth noting that an investigation of the critical nuclear charge for the $2p^2\ ^3P^e$ metastable bound state of two-electron atoms is also available in the literature [24,25].

Besides the numerical value of Z_c , the critical behavior of two-electron atoms around Z_c has attracted considerable interest in recent years. Ivanov [26] proposed that the ground-state energy of the two-electron atoms has a second-order pole at $Z_0 = 0$ and a third singular point at about $Z_2 \approx 0.106$. Based on the analytic properties, he successfully established a

*lgjiao@jlu.edu.cn

†aihualiu@jlu.edu.cn

dispersion relation which is remarkably useful in deriving an explicit form of the functional behavior of the imaginary part of the resonance energy in the close vicinity of Z_c [27,28]. In obtaining the benchmark value of Z_c , Estienne *et al.* [21] found that, before the ground state transforms into a shape resonance, the system wave function at the critical point is still square integrable and remains localized at a finite distance from the nucleus. Such a conjecture was confirmed by King *et al.* [29] in their calculations of the inner- and outer-electron radial density distribution functions. At the critical nuclear charge, the inner electron experiences a negative screening effect due to the perturbation of the outer electron, and eventually, its distribution closely resembles that of a hydrogenic atom, while the outer electron becomes very diffuse with a large mean radius. An investigation of electron radial distributions, correlation energies, Coulomb holes, and the finite nuclear mass effect in either the fully correlated or Hartree-Fock framework is also available from their group [30–32]. It is worth mentioning that the Shannon entropy, which is a classical information-theoretic quantity to measure the extent and concentration of the electron density distribution, has been employed as a powerful tool in analyzing the critical behavior of two-electron atoms. By calculating the one-electron density distribution from the two-electron wave function expressed in the Hylleraas basis set, Shi and Kais [33] predicted a steplike sharp increase of the Shannon entropy as the nuclear charge goes across Z_c , while Lin and Ho [34], using a similar but larger basis set, estimated a smooth and moderate increase of the Shannon entropy at Z_c . The smooth change in radial entropy manifests the fact that exactly at or in the vicinity of Z_c , the system wave function exhibits a localized behavior near the nucleus which is consistent with the predictions of Estienne *et al.* [21] and King *et al.* [29]. Recent interest in this system has been focused on the combined effect of varying the nuclear attraction and electronic screened Coulomb interaction as well as the possible existence of Borromean bound states due to their potential applications in plasma physics [35–41].

When $Z < Z_c$, where the system supports only quasi-bound shape-type resonances, the asymptotic behavior of the two-electron atoms is far from understood. A hypothetical trajectory of the resonance state in the complex-energy plane was proposed by Reinhardt [42] in 1977 in searching for the isolated bound state in the continuum. However, no solid conclusion can be drawn due to the lack of numerical calculations. Probably, the first explicit calculation of the complex resonance energies of two-electron atoms was performed by Dubau and Ivanov [28] for $1.11 \leq 1/Z \leq 1.14$ by using the complex-scaling method. It was shown that the resonance width follows very well the dispersion relation obtained by the authors based on the $1/Z$ expansion theory. In the subsequent work of Sergeev and Kais [43], the authors reproduced the numerical results of Dubau and Ivanov [28] by employing the complex stabilization method and proposed a one-particle Hellmann potential to qualitatively model the formation of resonances. However, such a simplified model works only in a range close to the critical nuclear charge. The most accurate prediction of the resonance energies is available from the recent complex-scaling calculation of Karr [23] for $0.905 \leq Z \leq 0.9103$. Based on the accurate numerical results, Karr

[23] validated the dispersion relation for the resonance width with a high degree of confidence. To the best of our knowledge, there are no other explicit calculations of the resonance states available in the literature for nuclear charge lying below the critical value, although in some interesting works [34,40,44] the variational methods were extended to a lower region where well-defined resonances are expected to survive. Nevertheless, the complete trajectory of the resonance states in the complex-energy plane is still a mystery.

In this work, we undertake a systematic investigation of the shape resonances in two-electron atoms to figure out the undiscovered critical behavior of resonances when the nuclear charge lies far below the critical value. The present paper is organized as follows. Section II presents a brief introduction of the basis functions used in the expansion of system wave functions and the variational (complex-scaling) method in the calculation of bound (resonance) states. Section III analyzes the variation of bound and resonance states, respectively, for nuclear charge above and below the critical value. For the former we focus on the bound property of the two-electron atoms in the vicinity of Z_c , while for the latter we discuss in detail the trajectory of the resonance pole in the complex-energy plane, the anomalous behavior of the resonance position, and the dispersion relation for the resonance width. Section IV gives the conclusion of this work. Atomic units are used throughout this paper unless otherwise specified.

II. THEORETICAL METHOD

The nonrelativistic Hamiltonian of the two-electron atom with infinitely heavy nuclear mass is given by

$$H = -\frac{1}{2}\nabla_1^2 - \frac{1}{2}\nabla_2^2 - \frac{Z}{r_1} - \frac{Z}{r_2} + \frac{1}{r_{12}}, \quad (1)$$

where Z is the nuclear charge and can be any positive fractional value in the present investigation. The explicitly correlated Hylleraas configuration-interaction (HyCI) basis functions are employed to expand the system wave function. They are constructed in a manner similar to the Slater-type orbital configuration-interaction (STOCI) basis sets, which are expressed in terms of the product of one-electron STOs but include further the power series of interelectronic coordinate r_{12}

$$\begin{aligned} \Psi(\vec{r}_1, \vec{r}_2) = & (1 - \hat{P}_{12}) \sum_{k=0}^{k_{\max}} \sum_{l_a, l_b=0}^{l_{\max}} \sum_{i, j} C_{a_i, b_j} r_{12}^k \phi_{a_i}(r_1) \phi_{b_j}(r_2) \\ & \times Y_{l_a, l_b}^{LM}(\hat{r}_1, \hat{r}_2) S^{S, M_S}(\sigma_1, \sigma_2), \end{aligned} \quad (2)$$

where $\phi(r)$ is the radial part of a one-electron STO,

$$\phi_{a_i}(r) = r^{n_{a_i}-1} e^{-\xi_{a_i} r}, \quad (3)$$

in which ξ is the nonlinear parameter to be optimized for each configuration state and the notation i denotes different STOs with the same angular momentum l . $Y_{l_a, l_b}^{LM}(\hat{r}_1, \hat{r}_2)$ and $S^{S, M_S}(\sigma_1, \sigma_2)$ are the two-electron coupled orbital angular momentum and total spin wave functions, respectively. C_{a_i, b_j} is the expansion coefficient. The inclusion of positive powers of the interelectronic coordinate plays a vital role in the system wave functions fulfilling the Kato cusp condition at the

two-electron coalescence. The use of $k_{\max} = 0$ just reduces the HyCI basis functions to the conventional STOCI ones developed in our previous works [45,46]. The simplest and most efficient way of constructing the HyCI basis set is to set $k_{\max} = 1$, provided that the largest angular momentum l_{\max} of coupled STOs is large enough [47]. The multipole expansion of r_{12} in terms of Legendre polynomials, $r_{<}$ and $r_{>}$ [where $r_{<} = \min(r_1, r_2)$ and $r_{>} = \max(r_1, r_2)$], accounts at least in part for the coupling of higher-lying angular momenta [48]. The computation of the Hamiltonian and overlap matrix elements is similar to that for the Hylleraas basis set due to the explicit appearance of r_{12} . The computational methods developed by Drake [49,50] and Yan and Drake [51] can be applied very well to the present two-electron systems.

The advantages and disadvantages of the HyCI basis set compared to the original Hylleraas or STOCI basis sets have been extensively discussed in the literature, and interested readers are referred to the detailed discussion in Ref. [47]. In the present work, the Rayleigh-Ritz variational and complex-scaling [52] methods are employed, respectively, to estimate the eigenenergies of bound and quasibound resonance states for different nuclear charges. In the framework of complex scaling, or, more specifically, the complex-coordinate rotation [53], all radial coordinates in the Hamiltonian are rotated by an angle θ , i.e.,

$$r_j \rightarrow r_j e^{i\theta}, \quad j = 1, 2, 12. \quad (4)$$

The resulting Hamiltonian matrix $H(\theta)$ is therefore complex symmetric but not Hermitian. After resolving the energy spectra of the rotated Hamiltonian, the resonance pole is exposed by the rotated continuum cuts with a complex energy given by

$$E_{\text{res}} = E_r + iE_i \equiv E_r - i\frac{\Gamma}{2}, \quad (5)$$

where E_r is the resonance position and Γ is the total width, provided that θ is larger than $\arg(E_{\text{res}})/2$.

The two-electron HyCI functions used in the present variational and complex-scaling calculations are constructed in the same way but optimized differently. We first use two groups of STOs to form a near-complete one-electron basis, with each group sharing the same parameter ξ . Suppose the maximum principal quantum numbers of STOs in the first and second groups are n_1 and n_2 , respectively; then all possible orbitals with angular momenta $l_1 (<n_1)$ and $l_2 (<n_2)$ in the first and second groups are coupled together to build the two-electron configuration state function. Finally, the entire CI basis set is doubled by setting $k_{\max} = 1$, where the second set is additionally multiplied by r_{12} . Such a HyCI basis set is labeled by $(n_1, n_2)k_{\max}$. By systematically increasing n_1 and n_2 the convergence of calculations can be estimated, although the nearly linear dependence in the basis set will become more serious. Like other explicitly correlated basis functions, HyCI suffers more from the linear dependence problem due to some double counting of radial and angular couplings in the wave functions, or, from the viewpoint of the wave function, overlapping in the configurational spaces. In our previous work [54,55], Löwdin's canonical orthogonalization method [56] was shown to be a powerful method in reconstructing the nonorthogonal basis functions into orthogonal ones and simultaneously removing the redundant part of the basis set in

an optimal way. This method is employed here to refine the HyCI basis set.

In the Rayleigh-Ritz variational calculation of the ground state, only two parameters, ξ_1 and ξ_2 , are need to be optimized independently. The Bound Optimization BY Quadratic Approximation (BOBYQA) algorithm [57] for bound constrained optimization without derivatives is found to be very efficient. Since all numerical calculations are performed in real space and only the lowest eigenvalue of the Hamiltonian is required, we use an efficient inverse-iteration method [58] to solve the generalized symmetric eigenvalue problem. In the complex-scaling calculation, however, the situation becomes more complicated because one has to locate the most stabilized energy in the complex-energy plane by varying both the basis set and rotational angle. In doing so, we tentatively set $\xi_1 = \alpha$ and $\xi_2 = \alpha/n_1$ to evenly distribute the two groups of STOs. For each resonance state, the optimized values of the scaling parameter α_{opt} and rotational angle θ_{opt} are determined formally by [53]

$$\left| \frac{\partial E_{\text{res}}}{\partial \theta} \right|_{\alpha=\alpha_{\text{opt}}} = \min, \quad \left| \frac{\partial E_{\text{res}}}{\partial \alpha} \right|_{\theta=\theta_{\text{opt}}} = \min. \quad (6)$$

However, as we will show in the following, the above conditions are not easily satisfied in practical calculations due to the *incompleteness* of the truncated HyCI basis set employed here, and for this reason, careful attention is needed in locating the resonance pole.

III. RESULTS AND DISCUSSION

A. Bound states

To test the flexibility and accuracy of the HyCI basis set, we first calculate the ground-state energies of two-electron atoms with nuclear charge in the range $Z_c \leq Z \leq 1$, where the system is still bound and the Rayleigh-Ritz variational method can be applied. Because we solve the eigenvalue problem by using an inverse-iteration algorithm, all basis functions in the HyCI basis set must be retained in each iteration. All numerical calculations are performed in quadruple-precision arithmetic (≈ 34 digits after the decimal point). The largest basis set which is stable for all Z 's investigated here is (9,10)1, and it produces a total of 1320 terms in the expansion of system wave functions in the $^1S^e$ symmetry. The calculated results and a detailed comparison with other state-of-the-art theoretical predictions are included in Table I at selected values of Z .

For $Z = 1$, i.e., the H^- anion, our result differs from the benchmark value existing in the literature [50,59–61] by 9.7×10^{-14} a.u. Keeping in mind that the HyCI basis set employed here has only two independent variational parameters and the number of terms is restricted to 1320, the flexibility of the constructed basis set in representing this loosely bound system is noticeable. The fast convergence of the present calculations can be estimated by comparing the (9,10)1 result with those of the smaller basis sets (8,9)1, (8,10)1, and (9,9)1, whose total numbers of terms are 960, 1032, and 1230, respectively.

With continuously decreasing Z , the interelectronic correlation effect makes a larger contribution to the system Hamiltonian, and the accuracy of the present calculation

TABLE I. The ground-state energies of the two-electron atoms for selected values of Z above the critical nuclear charge Z_c calculated by using the Ritz variational method based on HyCI basis set (9,10)1. I_e represents the ionization energy.

Z	E	I_e
1.0 (8, 9)1	-0.52775101654188	
1.0 (8,10)1	-0.52775101654271	
1.0 (9, 9)1	-0.52775101654339	
1.0 (9,10)1	-0.52775101654428	2.77510(-2)
	-0.527751016544377 ^a	
	-0.52775101654438 ^b	
	-0.52775101654 ^c	
	-0.5277510151 ^d	
	-0.527751013 ^e	
0.98	-0.5008471800378	2.06472(-2)
	-0.50084718003 ^c	
	-0.5008471781 ^d	
0.95	-0.4621246996833	1.08747(-2)
	-0.4621246996838 ^b	
	-0.46212469967 ^c	
	-0.4621246954 ^d	
	-0.462124697 ^e	
0.92	-0.425485281672	2.28528(-3)
	-0.425485281676 ^b	
	-0.4254852816 ^c	
	-0.4254852567 ^d	
	-0.42548527 ^e	
0.912	-0.416111395518	2.39396(-4)
0.9111	-0.415069209902	1.76049(-5)
0.91103	-0.414988265855	4.35405(-7)
0.911029	-0.414987109633	1.90213(-7)
0.9110283	-0.414986300280	1.8580(-8)
0.91102823	-0.414986219345	1.417(-9)
0.911028225	-0.414986213564	1.91(-10)
0.9110282245	-0.414986212986	6.8(-11)
0.9110282244	-0.414986212870	4.4(-11)
0.9110282243	-0.414986212755	1.9(-11)
	-0.4149862128 ^c	
0.9110282242	-0.414986212639	-5(-12)
	-0.4149862126 ^c	
Z_c	-0.41498621251	
	-0.414986212532679 ^f	
	-0.41498621253 ^b	
0.911028223	-0.41498621125	
0.91102822	-0.41498620778	
0.9110282	-0.41498618466	
0.911028	-0.41498595342	
0.91102	-0.41497670379	
0.9110	-0.41495358070	
0.9103	-0.41414514955	
	-0.41414514963839 ^g	$E_i=-3.9(-14)$
0.910	-0.41379921115	
	-0.41379921124956 ^g	$E_i=-3.97(-12)$
	-0.4137989542 ^d	
	-0.413799 ^e	

^aDrake [50], Frolov [59], Nakashima and Nakatsuji [60], and Aznabaev *et al.* [61].

^bOlivares-Pilón and Turbiner [22].

^cKar *et al.* [38].

^dLin and Ho [34].

^eSadhukhan *et al.* [40].

^fEstienne *et al.* [21].

^gKarr [23].

is slightly reduced. At the critical value Z_c , our result is larger than the most accurate calculation of Estienne *et al.* [21] by 2.3×10^{-11} a.u. Actually, the critical nuclear charge where the ionization energy of the outer electron becomes zero predicted under the present HyCI basis set is about 0.9110282242, which is accurate to nine digits. For the two-electron systems between $Z = 1$ and Z_c , Olivares-Pilón and Turbiner [22] reported a very accurate estimate of the ground-state energy by employing the Lagrange-mesh method. The exponentially correlated basis calculations of Kar *et al.* [38] are generally on the same level of accuracy as ours. The predictions of Lin and Ho [34] and Sadhukhan *et al.* [40] based on Hylleraas wave functions are less accurate in the last few digits.

It has been shown by many authors that exactly at Z_c , the two-electron system is still bound and the inner electron [whose density distribution can be obtained by calculating $\rho(r_-)$] can be considered as in the hydrogenic $1s$ orbital and the outer electron [which is characterized by $\rho(r_+)$] remains localized near the nucleus. Then for $Z < Z_c$, the bound state changes smoothly into a shape resonance lying above the $Z(1s)$ threshold. However, when Z is very close to Z_c from below, the resonance width is so small that the system can still be treated as in a bound state due to its extremely long lifetime. At $Z = 0.9103$, for example, the calculation of Karr [23] based on Sturmian wave functions in perimetric coordinates successfully predicted the resonance energy with an imaginary part of -3.9×10^{-14} a.u. When Z increases from 0.9103 to Z_c , the magnitude of imaginary resonance energy decreases exponentially to zero, and extraction of its quantity from a limited-accuracy numerical calculation is a formidable task. Also shown in Table I are the present variational calculations of the lowest eigenenergy for $Z < Z_c$. Our calculation based on the HyCI basis set is generally accurate within 10 digits, and this is why the imaginary part of the resonance energy for $0.910 < Z < Z_c$ cannot be detected in the present work [$E_i(0.910) = -3.97 \times 10^{-12}$ a.u.]. Even so, our prediction of the *bound-state* energy agrees fairly well with the real part of the resonance energy in the complex-scaling calculation by Karr [23]. The variational calculations by Lin and Ho [34] and Sadhukhan *et al.* [40] for $Z < Z_c$ are supposed to be feasible for the same reason. Their results are generally accurate to six digits at $Z = 0.910$, so the small imaginary part is totally covered up by the numerical uncertainties. In the latter work, the authors extended the variational calculations for Z as small as 0.80, and in such a situation the convergence is further suppressed due to the non-negligible resonance width.

B. Resonance states

For $Z \leq 0.910$, the complex-scaling method is applied to extract the resonance energy. The HyCI basis sets (10,11)1 and (11,11)1 are employed in the present calculations, and they are coupled to a total number of 1760 and 2156 terms, respectively, in the expansion of system wave functions. For such large basis sets, Löwdin's canonical orthogonalization method [56] is employed to overcome the serious linearly dependent problem. The truncation threshold is set to be $\varepsilon = 10^{-20}$ (interested readers are referred to Ref. [54] for the exact meaning of the truncation threshold), and the basis

sets will generally be reduced by 8%–15% according to the scaling parameters used. The complex-scaling calculations are performed for a large number of scaling parameters ($\alpha = 0.6$ – 1.4) with different rotational angles ($\theta = 0.3$ – 0.9). Their optimized values are determined by Eq. (6), where the most stabilized resonance pole can be located.

Our numerical results are included in Tables II and III at some selected values of nuclear charge. The variations of the real and imaginary parts of the resonance energy with respect to Z are depicted in Figs. 1(a) and 1(b), respectively. To the best of our knowledge, the smallest nuclear charge whose resonance energy has been predicted in the literature is $Z = 0.80$. A detailed comparison with all previous works is summarized in Table II. The most accurate prediction of the resonance energy comes from the complex-scaling calculations of Karr [23] based on Sturmian wave functions in perimetric coordinates. Such a basis set does not suffer from the linear dependence problem due to the orthogonality of the Sturmian wave functions, and therefore, extremely large basis sets (several hundreds of thousands of terms) can be used. Resonance energies with 14 converged digits were reported by the author for $0.905 \leq Z \leq 0.9103$. Our calculations show full agreement with these results for the leading 10 digits after the decimal point in the real part and 9 digits in the imaginary part. Another complex-scaling calculation comes from Dubau and Ivanov [28] for $1/1.14 \leq Z \leq 1/1.11$, and their results were verified by Sergeev and Kais [43], who employed the complex stabilization method. From the comparison at $Z = 1/1.11$, our result clearly shows better agreement with the benchmark prediction of Karr [23]. Three variational calculations have also been performed for $Z < Z_c$. The physical reason for the application of variational methods in this region was discussed above. The drawbacks of these methods are obvious, e.g., the lack of prediction of the resonance width and the continuous loss of accuracy as the nuclear charge is further decreased. For $Z < 0.80$, no comparison can be made, and we tabulate only our results in Table III. The convergence of our calculations is also slower at smaller values of Z due to the increasingly large contribution of the electron correlation. At $Z = 0.26$, the resonance energy can be determined to only four digits even with the (11,11)1 basis set.

For illustrative purposes, we show in Fig. 2 the trajectories of the resonance energy of the system at $Z = 0.80$, 0.381 , and 0.316 in the complex-energy plane with respect to changing the basis-set parameter α and rotational angle θ . Those in Figs. 2(a) and 2(b) are, respectively, the complex resonance energies at $Z = 0.80$ for fixed values of θ (with varying α) and fixed values of α (with varying θ). Figures 2(c) and 2(d) are the same as Fig. 2(a), but for $Z = 0.381$ and 0.316 . Due to the truncated and thus *incomplete* nature of the HyCI basis sets used in the present work, the stabilization conditions shown in Eq. (6) cannot be completely fulfilled. We can observe only a stabilized behavior of the rotated eigenenergies around the resonance pole. All resonance energies reported in Tables II and III are determined by locating the central point, and as a result, the last digits may have rounding-off errors.

The systematic variations of the real and imaginary parts of the resonance energy predicted in this work are shown in Figs. 1(a) and 1(b), respectively. For a better view of the contribution of the electron correlation effect at different

TABLE II. The complex resonance energies of the two-electron atoms for selected values of Z below the critical nuclear charge Z_c calculated by using the complex-scaling method based on HyCI basis set (10,11)1.

Z	E_r	E_i
0.910	−0.4137992113 −0.41379921124956 ^a −0.4137989542 ^b −0.4137992 ^c −0.413799 ^d	≈0 −3.97(−12) ^a
0.9098	−0.4135687676 −0.41356876751044 ^a	−6(−11) −3.187(−11) ^a
0.9095	−0.4132233803	−5(−10)
0.909	−0.4126484991 −0.41264849904865 ^a −0.4126485 ^c	−4.7(−9) −4.46020(−9) ^a
0.9085	−0.4120746158 −0.41207461578607 ^a	−2.69(−8) −2.668457(−8) ^a
0.908	−0.4115017822 −0.41150178223000 ^a −0.411502 ^c	−9.93(−8) −9.9252439(−8) ^a
0.907	−0.4103594335 −0.41035943353204 ^a	−6.158(−7) −6.1554527(−7) ^a
0.906	−0.4092216332 −0.40922163330544 ^a	−2.0952(−6) −2.09507497(−6) ^a
0.905	−0.4080883006 −0.40808830062175 ^a −0.4081 ^c	−5.0977(−6) −5.09763393(−6) ^a
1/1.11	−0.4034828442 −0.40348284422335 ^a −0.403483 ^e −0.40351 ^f	−4.05593(−5) −4.05591446(−5) ^a −4.1(−5) ^e −4.9(−5) ^f
0.90	−0.4024778066 −0.4025301585 ^b −0.402971 ^d	−5.39585(−5)
1/1.12	−0.3945735586 −0.394574 ^e −0.39456 ^f	−2.281473(−4) −2.28(−4) ^e −2.23(−4) ^f
0.89	−0.3914371485 −0.3928805004 ^b −0.393854 ^d	−3.275253(−4)
1/1.13	−0.3859281753 −0.385928 ^e −0.38592 ^f	−5.369073(−4) −5.37(−4) ^e −5.48(−4) ^f
0.88	−0.3805476120 −0.3837953968 ^b −0.384855 ^d	−7.784237(−4)
1/1.14	−0.3775130734 −0.377513 ^e −0.37750 ^f	−9.286718(−4) −9.29(−4) ^e −9.31(−4) ^f
0.87	−0.369778680 −0.375957 ^d	−1.351105(−3)
0.85	−0.348582232 −0.358467 ^d	−2.733932(−3)
0.80	−0.297672438 −0.316508 ^d	−6.840979(−3)

^aKarr [23] complex-scaling method with perimetric coordinates.

^bLin and Ho [34] variational method with the Hylleraas basis.

^cTurbiner and Lopez Vieyra [44] Lagrange-mesh method.

^dSadhukhan *et al.* [40] variational method with the Hylleraas basis.

^eSergeev and Kais [43] complex stabilization method.

^fDubau and Ivanov [28] complex scaling with the Laguerre-CI basis.

TABLE III. Same as Table II, but for selected values of Z below 0.80. Calculations for Z above and below 0.32 are performed on HyCI basis sets (10,11)1 and (11,11)1, respectively.

Z	E_r	E_i	Z	E_r	E_i	Z	E_r	E_i
0.80	-0.297672438	-0.006840979	0.42	-0.0320208	-0.0239524	0.32	-0.000874	-0.019405
0.75	-0.250025756	-0.011121537	0.41	-0.0281817	-0.0237016	0.317	-0.00019	-0.01920
0.70	-0.20594040	-0.01511703	0.40	-0.0245051	-0.0234055	0.316	0.00005	-0.01913
0.65	-0.16563025	-0.01858290	0.39	-0.0209909	-0.0230640	0.315	0.00027	-0.01906
0.60	-0.12924737	-0.02136003	0.381	-0.017966	-0.022718	0.31	0.00136	-0.01870
0.55	-0.09689721	-0.02332803	0.38	-0.017638	-0.022677	0.30	0.00345	-0.01796
0.50	-0.0686457	-0.0243845	0.37	-0.014446	-0.022245	0.29	0.00540	-0.01718
0.48	-0.0585003	-0.0245309	0.36	-0.011413	-0.021765	0.28	0.00715	-0.01635
0.47	-0.0536754	-0.0245421	0.35	-0.008541	-0.021241	0.27	0.0088	-0.0155
0.45	-0.0445203	-0.0244371	0.34	-0.005827	-0.020673	0.26	0.0103	-0.0146

nuclear charges, we draw in the inset of Fig. 1(a) the Z -scaled resonance positions $E_r(Z)/Z^2$ and hydrogenic thresholds $-1/(2n^2)$, where n is the principal quantum number. It is

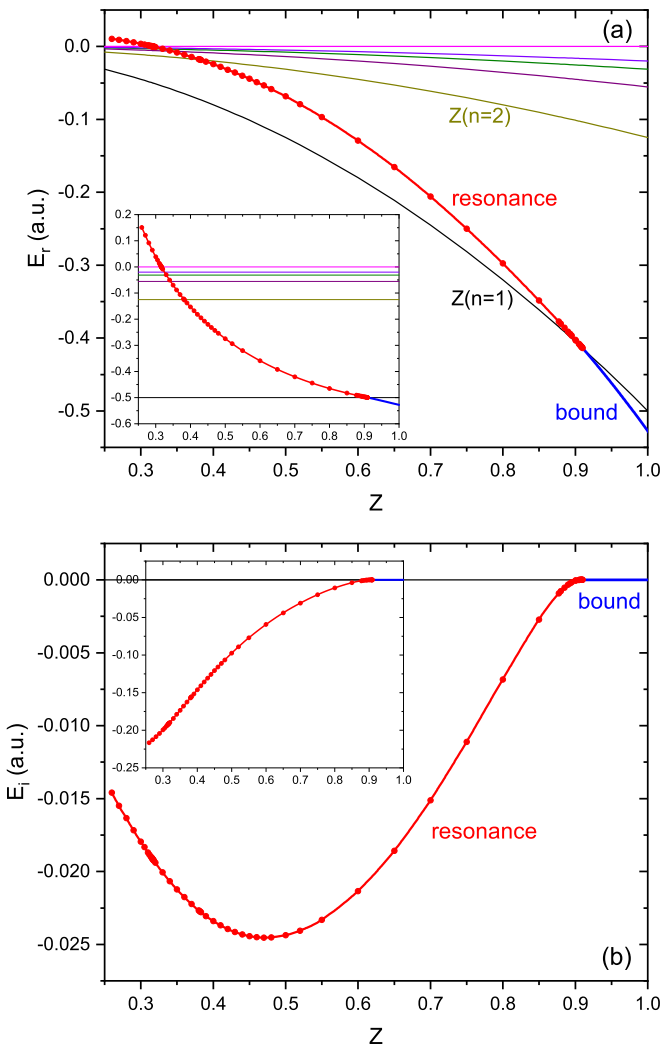


FIG. 1. The bound and resonance energies of the two-electron atoms as a function of nuclear charge Z . (a) Real part of the energies and (b) imaginary part of the energies. In each plot, the inset shows the variation of Z -scaled energies E/Z^2 as a function of Z . $Z(n)$ in (a) represents the threshold energy of a one-electron atom with principal quantum number n .

clearly seen that the resonance position increases rapidly and monotonically as the nuclear charge is decreased, while the imaginary part of the resonance energy first decreases, shows a minimum at about $Z = 0.472$, and then increases towards zero. An unexpected feature observed here is that at about $Z = 0.381$ the shape resonance will surpass the $Z(n = 2)$ threshold and, furthermore, at about $Z = 0.316$ it even lies above the zero energy, which is the three-body breakup threshold. We would like to discuss these phenomena from the following two aspects.

(i) The crossing of the shape resonance associated with a lower-lying threshold over higher-lying thresholds was observed in our previous investigation of the supermultiplet structures of intrashell resonances in H^- [45]. In such a negative-ion system, the $4f^2 \ ^1S^e$ shape resonance (which is also labeled by $4[-3, 0]_4$ in the more physical ${}_N[K, T]_n$ representation [62]) lies above the $H(n = 5)$ threshold (see Fig. 2(c) in Ref. [45] and the corresponding discussion for more details), and the $5g^2 \ ^1S^e$ shape resonance (labeled by $5[-4, 0]_5$) even lies above the $H(n = 7)$ threshold [63]. For such extremely high-lying shape resonances, the electron correlation effect plays a dominant role over the nucleus-electron attraction interaction, which is similar to the present situation. Decreasing the nuclear charge Z in the two-electron atoms results in a loose capture of the outer electron and manifests an effect similar to increasing the excitation (decreasing the K quantum number) of intrashell resonances in the $N = n$ series. A consequence is that one would not observe these higher-threshold-lying resonances or even the above-threshold shape resonances in the neutral He atom and any positive He-like ions where the nucleus-electron attraction dominates, resulting in all the above-threshold shape-type resonances being pushed down to lie below thresholds and to become Feshbach resonances. Therefore, it is not surprising that the $1s^2 \ ^1S^e$ shape resonance (which can alternatively be labeled by $1[0, 0]_1$) would lie above the $Z(n = 2)$ and even higher thresholds at very small values of Z , taking into account the increasingly important interelectronic interaction.

(ii) The existence of positive-energy shape resonances in the two-electron systems for $Z < 0.316$ is counterintuitive. To understand such anomalous behavior we seek help from the simplified model proposed by Estienne *et al.* [21]. When the outer electron is located far away from the residual ion, it experiences the combination of a long-range fully screened

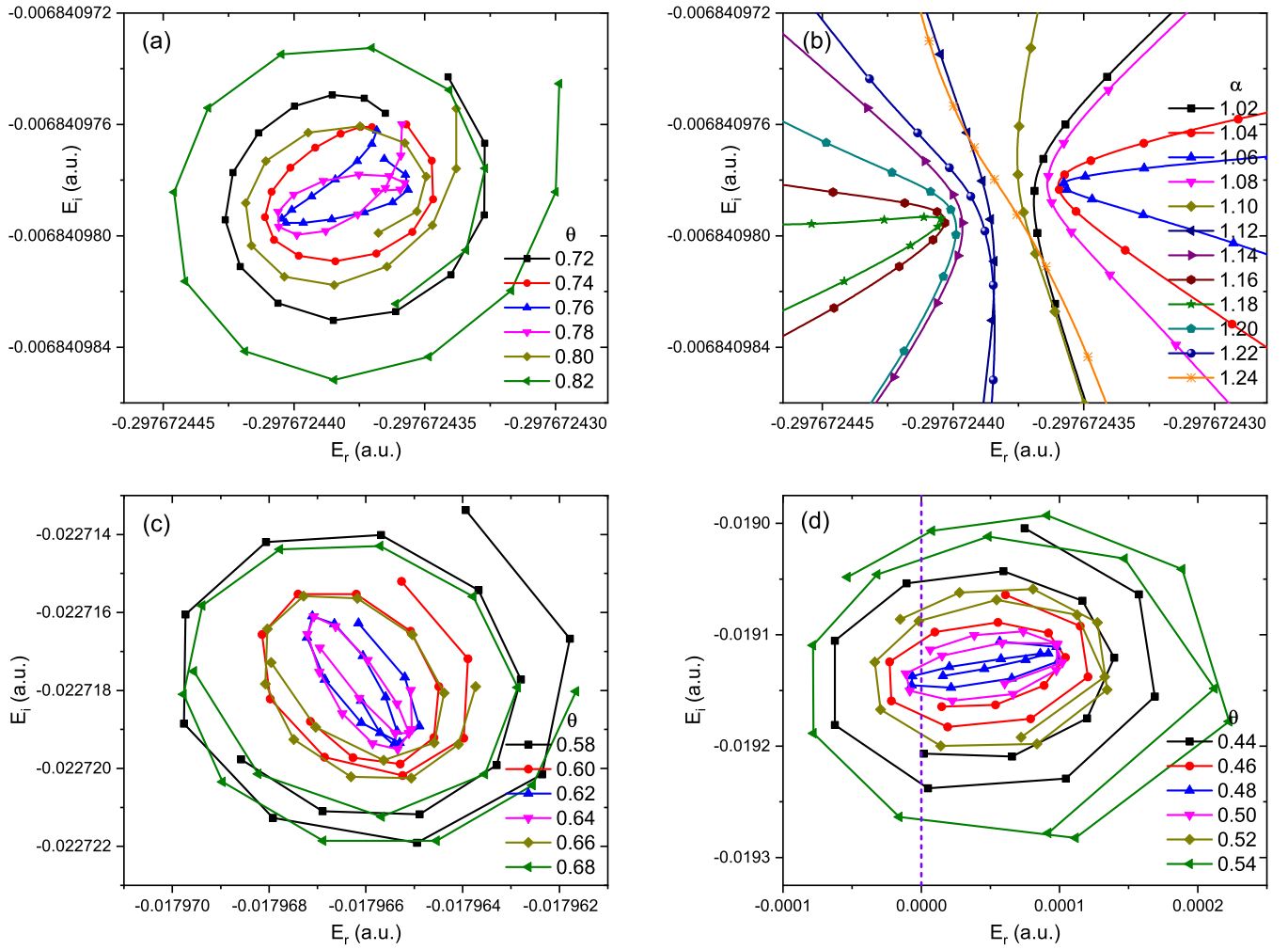


FIG. 2. The complex rotated eigenenergies of the system Hamiltonian at different values of rotational angle θ and scaling parameter α . Solid lines in (a), (c), and (d) are drawn at fixed values of θ with varying α , while in (b) they are at fixed values of α with varying θ . The resonance energy is expected to be located at the center of the rotated spectra. (a) $Z = 0.80$ with $\theta = 0.72$ – 0.82 and $\alpha = 1.02$ – 1.30 both at intervals of 0.02 , (b) $Z = 0.80$ with $\alpha = 1.02$ – 1.24 and $\theta = 0.70$ – 0.84 both at intervals of 0.02 , (c) $Z = 0.381$ with $\theta = 0.58$ – 0.68 and $\alpha = 0.70$ – 0.98 , and (d) $Z = 0.316$ with $\theta = 0.44$ – 0.54 and $\alpha = 0.68$ – 0.94 . The dashed line in (d) demonstrates the $E = 0$ three-body breakup threshold above which a well-isolated resonance is clearly observed.

Coulomb repulsion of the form $-(Z - 1)/r$ and a short-range attractive polarization potential which in the dipole approximation reads $-9/(4Z^4 r^4)$. The resulting model potential is

$$V(r) = -\frac{Z - 1}{r} - \frac{9}{4Z^4 r^4}. \quad (7)$$

It has both a potential well and a barrier which can capture the electron to form a resonance state with a finite lifetime before it escapes via tunneling. (However, this potential cannot be directly used in the numerical calculation of resonance energies because of the divergent $1/r^4$ term near the origin. A more physical model potential should not be more singular than $-Z/r^2$ at the origin.) The height of the potential barrier can be obtained by substituting

$$r_{\text{top}} = \left(\frac{9}{(1 - Z)Z^4} \right)^{1/3}, \quad (8)$$

which is obtained from $dV(r)/dr = 0$, into Eq. (7). In Fig. 3 we show a comparison of the resonance position, the $Z(n = 1)$

threshold energy, and the height of the model potential barrier. The variation of the resonance position shows qualitative agreement with the increase of the potential height, which demonstrates very well the physical nature of the origin of the shape resonance. At intermediate and large values of Z the resonance energy is found to be located above the threshold but below the height of the potential barrier. However, for $Z < 0.482$ the resonance position slightly surpasses the potential barrier, and for $Z < 0.316$ it lies above the zero energy. Such a phenomenon is probably related to the large width of the shape resonance. Based on the complex-scaling theory and the definition of Berggren [64], the real part of the complex expectation value of the Hamiltonian is treated as the resonance position, while its imaginary part contributes to the uncertainty of such an expectation value, which is due to the coupling of the resonance state to the continuum [65,66]. Therefore, a large resonance width would lead to a non-negligibly large variance of the distribution of the resonance position. A full understanding of this phenomenon

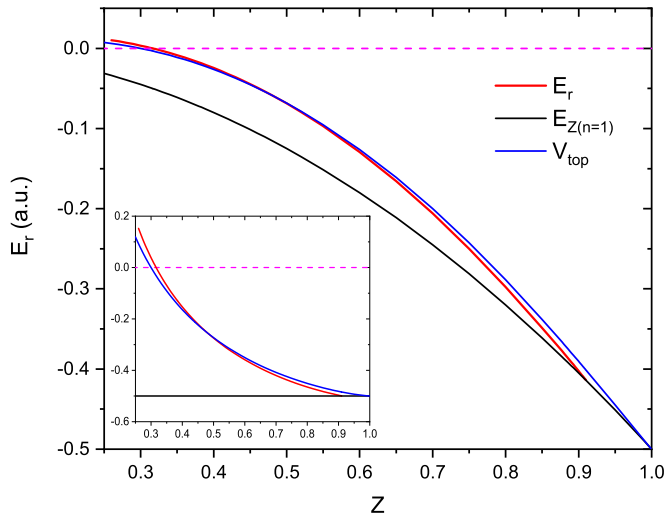


FIG. 3. Comparison among the resonance position, the autoionization threshold, and the top of the model potential barrier. E_r is the real part of the complex resonance energy, $E_{Z(n=1)}$ is the ground-state energy of the one-electron atom, and V_{top} represents the absolute height of the potential barrier including the threshold energy. The inset shows the corresponding Z -scaled energies as a function of Z .

still needs further rigorous theoretical consideration. From the scattering point of view, the existence of positive-energy shape resonances in the two-electron atoms is responsible for the modulation of ionization cross sections in the electron- (Z, e) atom scatterings. However, due to the near-threshold phenomena, a shape resonance with a large width would give a very broad and weak structure in the background cross sections [67], which makes it hard to detect from direct scattering calculations.

The unusual phenomenon of resonances lying above the ionization threshold can be reasonably related to the shape resonances in the realistic system of H^{2-} , which have attracted considerable interest for both theoretical and experimental aspects [53,68–73]. By using different theoretical methods, several authors [71,72] have shown that at least one 4S shape resonance lying above the $\text{H}(n=2)$ threshold exists. From a similar scattering analysis of the H^{2-} system and a comparison to the present two-electron atom with fractional nuclear charge, it is obvious that this resonance lies close to, but energetically above, the ionization threshold (breaking up into $[\text{H}(2p), e, e]$ pieces) in the electron- $\text{H}^-(2p^2) \ ^3P^e$ scatterings. A similar question raised in Refs. [68,72] is “Can we expect with certainty that this broad state close to the threshold is observable and how—and to what extent will the calculated property be related to the expected energy-dependent features of the resonance structure?” Such a common question does not have a certain answer yet.

It is also of great interest to trace the movement of resonance poles in the complex-energy plane with varying nuclear charge. This is shown in Fig. 4 together with an inset displaying the Z -scaled complex energies. The trajectory of the resonance in the complex momentum plane as the pole of the scattering S matrix [74] can be drawn correspondingly by utilizing the energy-conservation law $E_{\text{res}} = p^2/2 + E_{Z(n=1)}$, which is understood from the scattering of an electron with

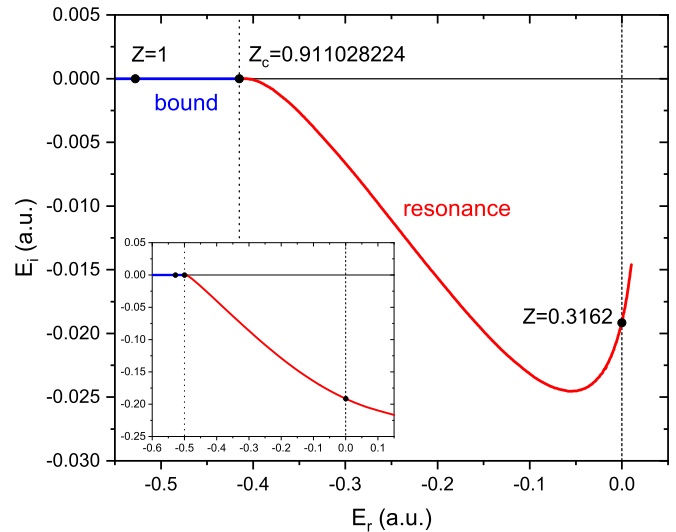


FIG. 4. Trajectory of the eigenvalue of the two-electron atoms in the complex-energy plane with decreasing Z . States for $Z < 0.3162$ are expected to be the positive-energy shape resonances with central positions lying above the three-body breakup threshold. The inset shows the trajectory of the Z -scaled eigenvalues.

momentum p from the one-electron system in the ground state. An attempt to depict a figure like Fig. 4 was made in 1977 by Reinhardt [42] in searching for the possible bound states embedded in the continuum. He proposed a hypothetical trajectory of the eigenvalue of the Z -scaled Hamiltonian $H(\theta)/Z^2$ in the complex-energy plane based on the dilatation analyticity of the complex-scaling transformation (see Fig. 3 in Ref. [42]). Reinhardt [42] also conjectured that the Z -scaled resonance energy would probably touch the $E_i = 0$ line at a single value of Z where a bound state in the continuum occurs between the threshold energies with a real-valued negative eigenenergy. From the inset in Fig. 4, it is clear that the trajectory of the resonance pole in the Z -scaled energy plane moves off the real axis monotonically and passes through all threshold energies including zero at about $Z = 0.3162$. In conjunction with the theorem proposed by Simon [75] that for an N -particle Coulomb system bound states in the continuum cannot occur for $E > 0$, we conclude that such a phenomenon would not appear in the two-electron Coulomb systems with any fractional nuclear charge.

Another interesting question raised here is about the full trajectory of the resonance pole for $Z > 0$. Due to the slow convergence of the present calculations at very small nuclear charges, little information is known in the region $0 < Z < 0.26$. Based on the Rayleigh-Schrödinger perturbation expansion of the ground-state energy in powers of $\lambda = 1/Z$, Stillinger [76] supposed $E(\lambda)$ has a second-order pole at $\lambda_\infty = \infty$ ($Z_0 = 0$) and also conjectured that another singular point which terminates the cut in the complex λ plane exists. These hypotheses were confirmed by Ivanov [26,27], who showed that $E(\lambda)$ has a third singular point at $\lambda_2 \approx 9.41$, i.e., $Z_2 \approx 0.106$. Unfortunately, we are not in a position to explore such a singular point in the present work. More sophisticated techniques, such as the complex-scaling method based on Sturmian wave functions in perimetric coordinates employed

by Karr [23], might be able to shed light on such an elusive region.

C. Dispersion relation for resonance width

Based on the analytic properties of the system energy as a function of nuclear charge and the asymptotic behavior of the expansion coefficients in the $1/Z$ perturbation expansion, Dubau and Ivanov [27,28] proposed a dispersion relation which connects the real part of the system energy for $Z > Z_c$ to the imaginary part of the system energy for $Z < Z_c$. For convenience, we will use $E'(Z) = E(Z)/Z^2$ in the following discussion. It was shown by the authors [27,28] that as Z approaches the critical point Z_c from below, the imaginary part of the resonance energy behaves as

$$\text{Im}E'(Z) \approx Ax^p e^{-\frac{c}{x}}, \quad (9)$$

where

$$x \equiv 1 - Z/Z_c. \quad (10)$$

The fitting parameters are given by

$$A \approx -13, \quad p = 2.2397, \quad c = 0.018446. \quad (11)$$

To extend the applicability of the formula shown above for Z moving away from Z_c , one must include higher-order corrections which are expressed in a series expansion over x

$$\text{Im}E'(Z) = Ax^p e^{-\frac{c}{x}} (1 + e_1 x + e_2 x^2 + \dots). \quad (12)$$

The parameter e_1 can be analytically obtained [28] and acquires the significantly large value of $e_1 \approx -123$ due to the presence of a small parameter c in the exponent. The large magnitude of e_1 leads to slow convergence of the Taylor series even if x is small.

The Padé approximant method is known as a powerful technique to improve the convergence properties of the Taylor series and extend the convergence radius [77,78]. Dubau and Ivanov [28] adopted the simplest Padé[0,1] approximant, which reads

$$\text{Im}E'(Z) = Ax^p e^{-\frac{c}{x}} \frac{1}{1 - e_1 x}. \quad (13)$$

They showed that for $0.011 < x < 0.037$ the Padé[0,1] approximant considerably improves the agreement between numerically calculated imaginary resonance energies and values predicted using the above approximate formula.

With higher-accuracy imaginary resonance energies obtained in a region closer to Z_c , Karr [23] further examined the dispersion relation at smaller values of x ($0.001 < x < 0.007$). It was found that by further taking Z_c as a fitting parameter (Z^*), the complex-scaling calculation shows very good agreement with the dispersion relation in Eq. (9) with parameters

$$p = 2.42, \quad c = 0.0180, \quad Z^* = 0.911276. \quad (14)$$

The unreported value of A probably is -14.68 , which we obtained by repeating Karr's fitting procedure. Considering that the fitting performed by Karr [23] was primarily focused on the region near Z_c , where the imaginary resonance energies are extremely small, and that the uncertainties in other fitting

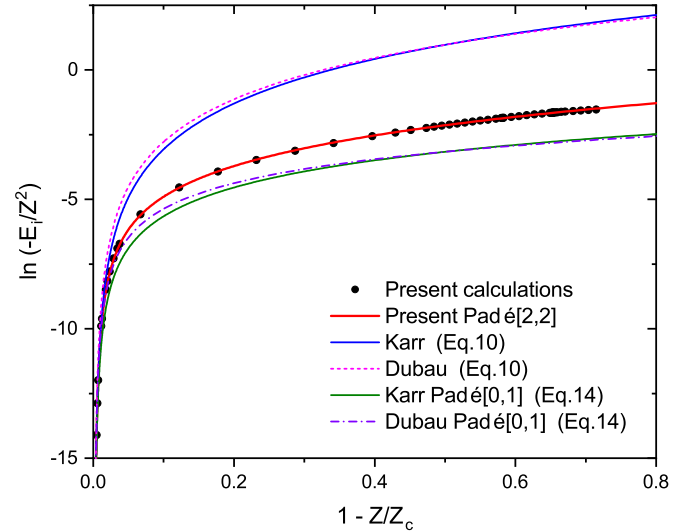


FIG. 5. Fitting of the numerical calculation of the imaginary part of the resonance energies as a function of $1 - Z/Z_c$. The fitting parameters obtained by Karr [23] and Dubau and Ivanov [28] are given in Eqs. (11) and (14), respectively. Padé[M, N] represents the improved asymptotic law of Eq. (15), which includes the correction of Padé[M, N] approximants.

parameters are quite large, the small difference between Z_c and Z^* is reasonably acceptable.

In Fig. 5, we display the applicability of the asymptotic formulas in Eqs. (9) and (13) at larger values of x , i.e., smaller Z . The use of either Z_c or Z^* in x does not change much in the figure. It is clearly seen that the leading-order formula in Eq. (9) significantly overestimates the imaginary part of the resonance energy, while the incorporation of the Padé[0,1] correction, on the contrary, underestimates the numerical results to a large extent. The use of different fitting parameters listed in Eqs. (11) and (14) has a small effect at large x , although the latter performs better in the near-zero region (see Fig. 1 in Ref. [23]). In the present work, we perform a different fitting formula by incorporating the higher-order Padé[M, N] correction, which yields

$$\text{Im}E'(Z) = Ax^p e^{-\frac{c}{x}} \frac{\sum_{k=0}^M a_k x^k}{1 + \sum_{k=1}^N b_k x^k}. \quad (15)$$

The parameters given by Karr [23] are used for p , c , and Z^* . Other parameters used in the present work are $A = -14.68$, $a_0 \equiv 1$, and $b_1 \equiv -e_1 = 123$. It is found that the lowest order of Padé approximant which can reproduce the numerical calculations in the entire x region investigated here fairly well is Padé[2,2] (see Fig. 5). The corresponding coefficients read $a_1 = 165.8$ and $a_2 = 146.5$, which are the same magnitude as b_1 , while $b_2 = 10560$ is two orders of magnitude larger than the others. These parameters may vary if one uses the parameters in Eq. (11) or employs a higher-order Padé approximant. It is worth noting that the fitting procedure adopted here is quite different from the usual application of Padé approximants, where one first calculates the coefficients of the Taylor expansion [e.g., e_n in Eq. (12)] and then solves the linear equations iteratively to get the Padé coefficients [77]. When Eq. (12) is directly used in the fitting process, it is

found that e_2 is one order of magnitude larger than e_1 and so forth between e_n and e_{n-1} , which is in qualitative agreement with the prediction of Dubau and Ivanov [28]. Considering the divergent behavior of the expansion coefficients, the usual procedure is a formidable task in the present case.

IV. CONCLUSION

In this work, we have performed systematic research on the shape resonances of two-electron atoms below the critical nuclear charge Z_c by employing the complex-scaling method based on explicitly correlated HyCI basis functions. For Z lying below but very close to Z_c , the imaginary part of the resonance energy is so small that one can still estimate the resonance position by employing conventional variational methods. However, when Z is decreased farther away from Z_c , the complex-scaling or similar methods are well developed to extract the resonance energy from the stabilization criteria.

We traced the variation of the shape resonance from Z_c down to very small values of Z and found that the resonance position will go across the hydrogenic $Z(n=2)$ thresholds at about 0.381 and even the three-body breakup threshold at about 0.316. The crossing of the shape resonance over higher-lying thresholds is attributed to the increasingly important role of the interelectronic correlation effect along with decreasing nuclear charge. The formation of shape resonances can reasonably be modeled by a simplified model potential containing both a static repulsive potential and an attrac-

tive dipole interaction. It is conjectured that the existence of positive-energy resonance is related to the large magnitude of the resonance width. We finally showed that the dispersion relation can be applied to estimate the asymptotic behavior of the imaginary resonance energy fairly well, but for smaller values of Z one must include higher-order corrections, e.g., through a higher-order Padé approximant.

We believe that the present conclusion about two-electron atoms with fractional nuclear charge could be extended to multielectron atomic and molecular systems, especially anions. It has been shown by many authors that the asymptotic behavior and stability of multielectron atoms near the critical region can be simulated by a one-electron model [13,43] which is similar to the one employed here and that the binding energy of the outermost electron can be expressed in terms of a Rydberg-like hydrogenic energy formula with an additional quantum defect [16,17]. Therefore, one may expect similar shape resonances crossing higher-lying thresholds or even the existence of positive-energy resonances in these loosely bound systems. Such investigations would provide new information in our understanding of the resonance structures and related scattering dynamics.

ACKNOWLEDGMENTS

Financial support from the National Natural Science Foundation of China (Grants No. 12174147, No. 11774131, and No. 91850114) is greatly appreciated.

-
- [1] M. Hoffmann-Ostenhof, T. Hoffmann-Ostenhof, and B. Simon, *J. Phys. A* **16**, 1125 (1983).
 - [2] P. Serra and S. Kais, *Phys. Rev. Lett.* **77**, 466 (1996).
 - [3] S. Kais and P. Serra, *Adv. Chem. Phys.* **125**, 1 (2003).
 - [4] E. P. Ivanova and U. I. Safronova, *J. Phys. B* **8**, 1591 (1975).
 - [5] J. D. Baker, D. E. Freund, R. N. Hill, and J. D. Morgan, III, *Phys. Rev. A* **41**, 1247 (1990).
 - [6] J. Zamastil, J. Čížek, L. Skála, and M. Šimánek, *Phys. Rev. A* **81**, 032118 (2010).
 - [7] A. V. Turbiner and J. C. Lopez Vieyra, *Can. J. Phys.* **94**, 249 (2016).
 - [8] J. W. Hollett and P. M. W. Gill, *J. Chem. Phys.* **134**, 114111 (2011).
 - [9] T. Uhlřřová and J. Zamastil, *Phys. Rev. A* **101**, 062504 (2020).
 - [10] H. G. A. Burton, *J. Chem. Phys.* **154**, 111103 (2021).
 - [11] H. E. Montgomery, Jr., K. D. Sen, and J. Katriel, *Chem. Phys. Lett.* **782**, 139030 (2021).
 - [12] H. Hogreve, *J. Phys. B* **31**, L439 (1998).
 - [13] A. V. Sergeev and S. Kais, *Int. J. Quantum Chem.* **75**, 533 (1999).
 - [14] N. L. Guevara and A. V. Turbiner, *Phys. Rev. A* **84**, 064501 (2011).
 - [15] J. Katriel, M. Puchalski, and K. Pachucki, *Phys. Rev. A* **86**, 042508 (2012).
 - [16] J. Katriel, G. Gaigalas, and M. Puchalski, *J. Chem. Phys.* **138**, 224305 (2013).
 - [17] J. Katriel, J. P. Marques, P. Indelicato, A. M. Costa, M. C. Martins, J. P. Santos, and F. Parente, *Phys. Rev. A* **90**, 052519 (2014).
 - [18] F. H. Stillinger and T. A. Weber, *Phys. Rev. A* **10**, 1122 (1974).
 - [19] I. A. Ivanov, *Phys. Rev. A* **51**, 1080 (1995).
 - [20] J. P. Neirotti, P. Serra, and S. Kais, *Phys. Rev. Lett.* **79**, 3142 (1997).
 - [21] C. S. Estienne, M. Busuttill, A. Moini, and G. W. F. Drake, *Phys. Rev. Lett.* **112**, 173001 (2014).
 - [22] H. Olivares Pilón and A. V. Turbiner, *Phys. Lett. A* **379**, 688 (2015).
 - [23] J.-Ph. Karr, *Phys. Rev. A* **92**, 042505 (2015).
 - [24] J. P. Neirotti, P. Serra, and S. Kais, *J. Chem. Phys.* **108**, 2765 (1998).
 - [25] Z.-C. Yan and Y. K. Ho, *J. Phys.: Conf. Ser.* **635**, 052015 (2015).
 - [26] I. A. Ivanov, *Phys. Rev. A* **54**, 2792 (1996).
 - [27] I. A. Ivanov and J. Dubau, *Phys. Rev. A* **57**, 1516 (1998).
 - [28] J. Dubau and I. A. Ivanov, *J. Phys. B* **31**, 3335 (1998).
 - [29] A. W. King, L. C. Rhodes, and H. Cox, *Phys. Rev. A* **93**, 022509 (2016).
 - [30] A. W. King, L. C. Rhodes, C. A. Readman, and H. Cox, *Phys. Rev. A* **91**, 042512 (2015).
 - [31] A. L. Baskerville, A. W. King, and H. Cox, *R. Soc. Open Sci.* **6**, 181357 (2019).
 - [32] A. W. King, A. L. Baskerville, and H. Cox, *Phil. Trans. R. Soc. A* **376**, 20170153 (2018).
 - [33] Q. Shi and S. Kais, *Chem. Phys.* **309**, 127 (2005).
 - [34] C.-H. Lin and Y. K. Ho, *Chem. Phys. Lett.* **633**, 261 (2015).
 - [35] Y. K. Ho, *JPS Conf. Proc.* **18**, 011027 (2017).
 - [36] K. D. Sen, J. Katriel, and H. E. Montgomery, Jr., *Ann. Phys. (NY)* **397**, 192 (2018).

- [37] H. E. Montgomery, Jr., K. D. Sen, and J. Katriel, *Phys. Rev. A* **97**, 022503 (2018).
- [38] S. Kar, Y.-S. Wang, and Y. K. Ho, *Phys. Rev. A* **99**, 042514 (2019).
- [39] S. Kar, Y.-S. Wang, Y. Wang, and Y. K. Ho, *Atoms* **7**, 53 (2019).
- [40] A. Sadhukhan, S. Dutta, and J. K. Saha, *Int. J. Quantum Chem.* **119**, e26042 (2019).
- [41] A. Sadhukhan, S. Dutta, and J. K. Saha, *Eur. Phys. J. D* **73**, 250 (2019).
- [42] W. P. Reinhardt, *Phys. Rev. A* **15**, 802 (1977).
- [43] A. V. Sergeev and S. Kais, *Int. J. Quantum Chem.* **82**, 255 (2001).
- [44] A. V. Turbiner and J. C. Lopez Vieyra, *Mod. Phys. Lett. A* **31**, 1650156 (2016).
- [45] L. G. Jiao and Y. K. Ho, *Phys. Rev. A* **89**, 052511 (2014).
- [46] L. G. Jiao and Y. K. Ho, *Phys. Rev. A* **90**, 012521 (2014).
- [47] L. G. Jiao, L. R. Zan, L. Zhu, Y. Z. Zhang, and Y. K. Ho, *Phys. Rev. A* **100**, 022509 (2019).
- [48] J. F. Perkins, *J. Chem. Phys.* **48**, 1985 (1968).
- [49] G. W. F. Drake, *Phys. Rev. A* **18**, 820 (1978).
- [50] G. W. F. Drake, *Springer Handbook of Atomic, Molecular, and Optical Physics* (Springer, New York, 2006).
- [51] Z.-C. Yan and G. W. F. Drake, *Chem. Phys. Lett.* **259**, 96 (1996).
- [52] W. P. Reinhardt, *Annu. Rev. Phys. Chem.* **33**, 223 (1982).
- [53] Y. K. Ho, *Phys. Rep.* **99**, 1 (1983).
- [54] L. G. Jiao and Y. K. Ho, *Int. J. Quantum Chem.* **115**, 434 (2015).
- [55] Y. Z. Zhang, Y. C. Gao, L. G. Jiao, F. Liu, and Y. K. Ho, *Int. J. Quantum Chem.* **120**, e26136 (2020).
- [56] P. O. Löwdin, *Adv. Quantum Chem.* **5**, 185 (1970).
- [57] M. J. D. Powell, Cambridge University, Report No. DAMTP 2009/NA06, 2009 (unpublished).
- [58] A. Lüchow and H. Kleindienst, *Comput. Chem.* **17**, 61 (1993).
- [59] A. M. Frolov, *Phys. Rev. E* **74**, 027702 (2006).
- [60] H. Nakashima and H. Nakatsuji, *J. Chem. Phys.* **127**, 224104 (2007).
- [61] D. T. Aznabaev, A. K. Bekbaev, and V. I. Korobov, *Phys. Rev. A* **98**, 012510 (2018).
- [62] D. R. Herrick, *Adv. Chem. Phys.* **52**, 1 (1982).
- [63] L. G. Jiao and Y. K. Ho (unpublished).
- [64] T. Berggren, *Nucl. Phys. A* **109**, 265 (1968).
- [65] A. Bürgers and J.-M. Rost, *J. Phys. B* **29**, 3825 (1996).
- [66] A. Bürgers, N. Brandefelt, and E. Lindroth, *J. Phys. B* **31**, 3181 (1998).
- [67] A. Bürgers and E. Lindroth, *Eur. Phys. J. D* **10**, 327 (2000).
- [68] T. Andersen, *Phys. Rep.* **394**, 157 (2004).
- [69] B. Peart and K. T. Dolder, *J. Phys. B* **6**, 1497 (1973).
- [70] L. H. Andersen, D. Mathur, H. T. Schmidt, and L. Vejby-Christensen, *Phys. Rev. Lett.* **74**, 892 (1995).
- [71] T. Sommerfeld, U. V. Riss, H.-D. Meyer, and L. S. Cederbaum, *Phys. Rev. Lett.* **77**, 470 (1996).
- [72] M. Bylicki and C. A. Nicolaides, *J. Phys. B* **31**, L685 (1998).
- [73] For a historical view of the debate on the existence of shape resonances in H^2^- , readers are referred to Refs. [53,68].
- [74] J. R. Taylor, *Scattering Theory: The Quantum Theory on Non-relativistic Collisions* (Wiley, New York, 1972).
- [75] B. Simon, *Math. Ann.* **207**, 133 (1974).
- [76] F. H. Stillinger, Jr., *J. Chem. Phys.* **45**, 3623 (1966).
- [77] W. H. Press, B. P. Flannery, S. A. Teukolsky, and W. T. Vetterling, *Numerical Recipes in FORTRAN 77* (Cambridge University Press, New York, 1992).
- [78] X. H. Ji, Y. Y. He, L. G. Jiao, A. H. Liu, and Y. K. Ho, *Phys. Lett. B* **823**, 136718 (2021).